1991ApJ...372..554A

THE ASTROPHYSICAL JOURNAL, 372:554–564, 1991 May 10
© 1991. The American Astronomical Society. All rights reserved. Printed in U.S.A.

MAGNETIC TWO-PHOTON SCATTERING AND TWO-PHOTON EMISSION: CROSS SECTIONS AND REDISTRIBUTION FUNCTIONS

S. G. ALEXANDER AND P. MÉSZÁROS
Department of Astronomy and Astrophysics, 525 Davey Laboratory, Pennsylvania State University, University Park, PA 16802
Received 1990 May 9; accepted 1990 August 24

ABSTRACT

We discuss the magnetic two-photon scattering cross section within the framework of quantum electrodynamics, and calculate explicitly the corresponding scattering redistribution function for this process and its inverse, as well as the scattering source function. We calculate in a similar way the magnetic two-photon emission process which follows the radiative excitation of Landau levels above ground. The two-photon scattering and two-photon emission are of the same order as the single-photon magnetic scattering. All three of these processes, and in optically thick cases also their inverses, are included in radiative transport calculations modeling accreting pulsars and gamma-ray bursters. These processes play a prominent role in determining the relative strength of the first two cyclotron harmonics, and their effects extend also to the higher harmonics.

Subject headings: gamma rays: bursts — line formation — pulsars — radiation mechanisms — stars: accretion — stars: magnetic — X-rays: binaries — X-rays: spectra

1. INTRODUCTION

The radiation spectra of accreting pulsars and gamma-ray bursters in the X-ray range are characterized and in many cases dominated by the resonant cyclotron scattering process. Cyclotron lines have recently been detected in a number of high-energy sources (Murakami et al. 1988; Clark et al. 1990; Nagase 1989), strengthening the validity of earlier data (Trümper et al. 1978; Mazets et al. 1982; White, Swank & Holt 1983). The modeling of the strength and shape of the observed cyclotron lines requires an accurate knowledge of the cross sections, including all the relevant processes that are necessary for a detailed radiative transfer calculation. Since the magnetic field is strong, $B \gtrsim 10^{12}$ G, and the typical electron energies in units of the electron rest mass are at least moderately high ($E/m_e c^2 \gtrsim 0.02$–0.1 when not higher), relativistic quantum effects must be taken into account. A quantum electrodynamics (QED) calculation of the single-photon scattering cross section in a strong magnetic field by nonperturbative methods was performed by Herold (1979), who calculated in some detail the process involving one photon in and one photon out, including in the intermediate state the possibility of excited cyclotron states, with the initial and final electrons assumed to be in the ground state, as shown in Figure 1*a* (here, and in the other figures, we omit showing the associated diagrams with the photon order exchanged, although they are included in the calculations). While for accreting pulsars these assumptions appeared initially reasonably appropriate, it was pointed out by Bussard & Lamb (1982) that in gamma-ray bursters one might want to consider the previous scattering process, but with the added possibility of the final electron being left in an excited state. This is also produced by a single-photon scattering process, but since the excited electron decays in an extremely short time, $t \sim 10^{-15}(B/10^{12}\ \mathrm{G})^{-2}$, a second photon (at $\omega \sim \omega_c = eB/mc$) is also produced (see Fig. 1*c*). The two-photon scattering is of the same order in the fine-structure constant ($\propto \alpha_f^2$) as the one-photon scattering, since both have two vertices where a real photon joins to a virtual electron propagator (*dashed line*). Notice that in the two-photon scattering the second final photon couples to a real (on the mass shell) electron excited (*solid line*), not to a virtual propagator, so a third factor of α_f does not enter. This is in contrast to the so-called double Compton scattering (Fig. 1*b*), which also has two final photons, but both of them are emitted simultaneously, so the second horizontal intermediate electron line is also a virtual propagator; thus there are three photon–virtual propagator vertices leading to a cross section proportional to α_f^3. This is a process which is one order higher in α_f compared with the single-photon and two-photon Compton scattering of Figures 1*a* and 1*c*, and can generally be neglected. By the same reasoning, it is obvious that in general two-photon scattering is as important as one-photon scattering. Near resonance, these processes become comparable to cyclotron absorption, which is a first-order process. The two-photon scattering process was calculated in QED by Bussard, Alexander, & Mészáros (1986, hereafter BAM) and Bussard, Mészáros, & Alexander (1985), who calculated the effects associated with the two final photons when the cross sections are averaged over a thermal distribution, and by Daugherty & Harding (1986), who considered the scattering cross sections with arbitrary final electron states. This process was also investigated in connection with the *Ginga* observations of the gamma-ray bursters GB 880205 and GB 870303 by Wang et al. (1989), using a nonrelativistic quantum mechanical formulation with relativistic dynamics, and by Harding & Preece (1989) and Alexander & Mészáros (1989), using the QED formulation. As pointed out by all these authors, the effect of the two-photon scattering is crucial in understanding the fact that the first and second harmonics observed in these objects are of comparable depth.

In this paper we investigate in detail the two-photon scattering process within the framework of QED, taking into account the normal-mode polarization structure of the magnetized plasma in which the photons propagate, and we discuss the related process of magnetic two-photon emission within the same formalism (see Fig. 1*d*). We point out that the two-photon emission process is of comparable importance to the two-photon scattering, since the two cross sections are of the same order. As pointed out by Melrose & Kirk (1986), who considered these processes in the neighborhood of the first resonance, the matrix elements of the two-photon emission and two-photon scattering are related by a crossing symmetry. While the two cross sections are closely related in the core, the former has no continuum. They strongly influence the cyclotron line spectral modeling, since the two-photon effects introduce a

© American Astronomical Society • Provided by the NASA Astrophysics Data System

1991ApJ...372..554A

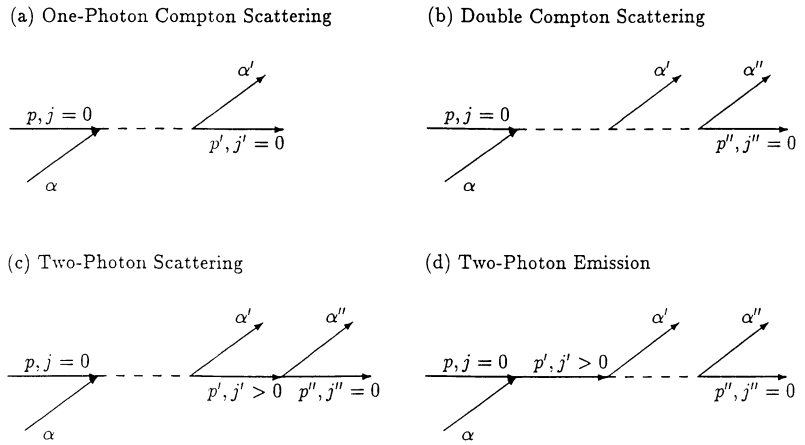

FIG. 1.—Diagrams for magnetic scattering processes. Electrons, shown as horizontal lines (solid for real; dashed for virtual), are represented by a momentum component p parallel to the external field and a total magnetic quantum number j. Photon states are designated by α and are incident from below the horizontal and are emitted above. The corresponding diagrams with permutation of photon order are not shown. Notice that processes (*c*) and (*d*) are compound, consisting of two successive Feynman graphs, for which two cross sections are calculated separately. The real propagator (*solid lines*) effectively decouples the two cross sections.

nonlinearity in the transfer equation which magnifies the effect of the cross sections (Alexander & Mészáros 1990a, b). Here we treat the relativistic two-photon scattering and emission cross sections in a general way, considering both the resonance and the continuum contributions, and we calculate the nonlinear redistribution function for a relativistic thermal electron distribution. These results are useful in order to perform detailed transfer calculations, either by Monte Carlo or by discrete ordinate difference equation methods. Model spectral calculations using these redistribution functions in the case of accreting pulsars and gamma-ray bursters (Alexander & Mészáros 1990b) are presented in the next paper.

In § 2 we discuss the one- and two-photon scattering and the two-photon emission cross sections, introducing the redistribution functions and the opacities and source terms corresponding to the various diagrams involved, and expressing all of them in terms of two redistribution functions $\mathscr{X}$ and $\mathscr{Y}$. In § 3 we specialize to the case of a relativistic thermal distribution, and calculate specific examples for typical magnetic fields, densities, and temperatures, comparing the opacities and sources for the scattering and emission processes. In § 4 we discuss the implications of these for radiative transfer calculations and models of X-ray pulsars and gamma-ray burst sources, with emphasis on the interpretation of cyclotron observations.

2. REDISTRIBUTION FUNCTIONS AND CROSS SECTIONS

2.1. *One-Photon Compton Scattering*

Define the Compton scattering redistribution function for an initial electron in state j as

$$\mathscr{R}_j(\alpha \to \alpha') \equiv \int dp\, n_j(p) \sum_{j'} \int dp' w_{jj'}(\alpha, p \to \alpha', p') , \tag{1}$$

where α denotes the set of photon parameters (ω = energy, μ = direction cosine relative to the external field, ϵ = polarization mode), and $n_j(p)$ is the distribution of electrons in magnetic state j with parallel momentum p. As was done in BAM, substitute the cross section from the Appendix, $w_{jj'}(\alpha, p \to \alpha', p')$; then the integrations over final and initial electron momenta can be performed. Also, if azimuthal symmetry is assumed, equation (1) can be integrated over the final photon azimuth, ϕ', and averaged over the initial photon azimuth, ϕ. This gives, for $\mathscr{R}_j(\alpha \to \alpha')$,

$$\mathscr{R}_j(\alpha \to \alpha') = \pi r_0^2 \frac{\omega'}{\omega} \sum_{j'} \sum_{p_\pm} n_j(p_\pm) \left[\frac{m^2(E+m)(E'+m)}{\{[\Delta + 2m\omega_c(j'-j)]^2 + 4\Delta(m^2 + 2m\omega_c j)\}^{1/2}} \right]_{p' = p+k-k'} \times \sum_{j''} \left[|a_{j''}|^2 + |b_{j''}|^2 + 2 \sum_{j_3} J_{j''+j_3-j'-j}(2\sqrt{\xi\xi'})\, \mathrm{Re}\,(a_{j''} b_{j_3}^*) \right] . \tag{2}$$

where $p_\pm$ are the two initial electron momenta allowed by energy and momentum conservation, and are

$$p_\pm = \frac{k'-k}{2\Delta} [\Delta + 2m\omega_c(j'-j)] \pm \frac{\omega'-\omega}{2\Delta} \{[\Delta + 2m\omega_c(j'-j)]^2 + 4\Delta(m^2 + 2m\omega_c j)\}^{1/2} , \tag{3}$$

where k designates the parallel component of the photon wavevector and $\Delta = (k'-k)^2 - (\omega'-\omega)^2$.

One-photon scattering is defined as Compton scattering with the initial and final electrons in the same state, which here will be taken to be the ground state, $j = j' = 0$ (Fig. 1*a*). Here and in what follows, the related diagrams with permutation of photons are not shown, but their effect is included in the computations. In problems of radiative transport that involve scattering, we must account for processes that scatter photons out of state α (in this paper referred to as opacity), and the inverse, i.e., processes that scatter

© American Astronomical Society • Provided by the NASA Astrophysics Data System

1991ApJ...372..554A

photons from all other states α' into α (in this paper referred to as sources). In terms of the redistribution function, the opacity, $\kappa_{C,\alpha}$, and the source, $Q_{C,\alpha}$, for one-photon Compton scattering are

$$\kappa_{C,\alpha} = \int d\alpha' \mathscr{R}(\alpha \rightarrow \alpha')(1 + N_{\alpha'}) , \tag{4}$$

$$Q_{C,\alpha} = \int d\alpha' N_{\alpha'} \mathscr{R}(\alpha' \rightarrow \alpha)(1 + N_{\alpha}) , \tag{5}$$

where $\mathscr{R}(\alpha \rightarrow \alpha')$ is the redistribution function for $j = j' = 0$, N_α is the occupation number of photons in α, and the integration over α' is shorthand for a summation over polarizations and integration over μ' and ω'. In this formulation the dimension of both the opacity and the source is that of cross sections (i.e., cm^2). The factors of $(1 + N_\alpha)$ account for stimulated scattering. These may be rewritten as in Alexander, Mészáros, & Bussard (1989) by using the condition of detailed balance and modifying for stimulated scattering to give

$$\kappa_{C,\alpha} = \int d\alpha' [1 + k_{st} N_{\alpha'}(1 - e^{(\omega' - \omega)/T})] \mathscr{R}(\alpha \rightarrow \alpha') , \tag{6}$$

$$Q_{C,\alpha} = \int d\alpha' N_{\alpha'} e^{(\omega' - \omega)/T} \mathscr{R}(\alpha \rightarrow \alpha') , \tag{7}$$

where k_{st} is a computational switch that equals 1 (0) to include (not include) stimulated effects, and a term proportional to N_α is treated as a negative opacity and included in $\kappa_{C,\alpha}$.

2.2 *Two-Photon Scattering*

As was seen in § 1, two-photon scattering occurs when the final electron state in the Compton process is an excited state. The electron then radiatively decays to give a second emitted photon. This compound process is given by the diagram in Figure 1*c* for the case of an initial ground-state electron, and the redistribution function for two-photon scattering can be constructed from the Compton scattering cross section and the cyclotron emission rate that are given in the Appendix. The general redistribution function is defined as

$$\mathscr{X}(\alpha \rightarrow \alpha'; \alpha'') \equiv \int dp\, n_j(p) \sum_{j'} \sum_{j'' < j'} \int dp' \frac{\int dp'' w_{jj'}(p, \alpha \rightarrow p', \alpha') w_{j'j''}(p' \rightarrow p'', \alpha'')}{\sum_{j''' < j'} \int d\alpha''' \int dp''' w_{j'j'''}(p' \rightarrow p''', \alpha''')} , \tag{8}$$

and is seen to be the integrated $j \rightarrow j'$ scattering cross section times the probability that the excited electron will radiatively decay with the emission of a particular photon α'', as opposed to any photon α'''. In this respect, the denominator should contain all of the possible decay modes; however, the direct emission rate will dominate. Note that this is a "one photon in, two photon out" redistribution. There is no significantly increased complexity, other than computational, in treating the next step in the hierarchy of multiple processes with one photon in, three out, e.g., when in Figure 1*c* or 1*d* the final electron is not yet $j'' = 0$ but, say, $j'' = 1$, which decays once more to give a third photon, which can occur if the incident photon has energy $\sim 3\omega_c$. For situations where the third harmonic is seen to be weak, this effect represents only a small correction, so we concentrate here on the two-photon processes. After the cross sections and rates are substituted in equation (8), the result can be integrated over final azimuth angles and averaged over initial ones. Also, the integrals over p' and p'' can be done with the delta functions, and the integral over p follows the same steps leading to equation (2). For the common case $j = j'' = 0$, this gives for the two-photon scattering redistribution function

$$\begin{aligned}\mathscr{X}(\alpha \rightarrow \alpha'; \alpha'') = \pi r_0^2 \frac{\omega'\omega''}{\omega} \sum_{j'} \sum_{p\pm} n_0(p_\pm) \frac{m^2(E + m)(E' + m)(E'' + m)}{[(\Delta + 2m\omega_c j')^2 + 4\Delta m^2]^{1/2} E''} \Bigg|_{\substack{p' = p + k - k' \\ p'' = p' - k''}} \\ \times \sum_{j_i} \left[|a_{j_i}|^2 + |b_{j_i}|^2 + 2 \sum_{j_3} J_{j_i + j_3 - j'}(2\sqrt{\xi\xi'})\, \mathrm{Re}\,(a_{j_i} b_{j_3}^*) \right] \\ \times \delta(E'' + \omega'' - E') |\boldsymbol{\epsilon}''^* \cdot \boldsymbol{G}_{\beta''\beta'}(-\boldsymbol{k}_\perp'')|^2 \Bigg/ \left[\sum_{j''' < j'} \sum_{\boldsymbol{\epsilon}'''} \int_{-1}^{1} d\mu''' \frac{\tilde{\omega}(E''' + m)}{E'''} |\boldsymbol{\epsilon}'''^* \cdot \boldsymbol{G}_{\beta'''\beta'}(-\tilde{\boldsymbol{k}}_\perp)|^2 \right] ,\end{aligned} \tag{9}$$

where here j_i denotes the intermediate virtual electron states, and in the denominator the decay frequency, $\tilde{\omega}$, is given by

$$\tilde{\omega} = \frac{(E' - p'\mu''') - [(E' - p'\mu''')^2 - 2m\omega_c j'(1 - \mu'''^2)]^{1/2}}{(1 - \mu'''^2)} , \tag{10}$$

and $E''' = E' - \tilde{\omega}$, by energy conservation.

If the two-photon scattering process is to be included in a radiative transfer calculation, we must include not only the direct process as in Figure 1*c* but also the inverse and exchange processes. This gives rise to three opacity and three source terms. With the aid of the detailed balance conditions between the individual scattering cross sections, we will show that all of the opacities and sources may be expressed as integrals over $\mathscr{X}(\alpha \rightarrow \alpha'; \alpha'')$. For a $j = 0 \rightarrow j'$ scattering and its inverse $j = j' \rightarrow 0$, the condition of detailed balance is

$$\bar{N}_\alpha n_0(p) w_{0j'}(p, \alpha \rightarrow p', \alpha')(1 + \bar{N}_{\alpha'}) = \bar{N}_{\alpha'} n_{j'}(p') w_{j'0}(p', \alpha' \rightarrow p, \alpha)(1 + \bar{N}_\alpha) , \tag{11}$$

© American Astronomical Society • Provided by the NASA Astrophysics Data System

1991ApJ...372..554A

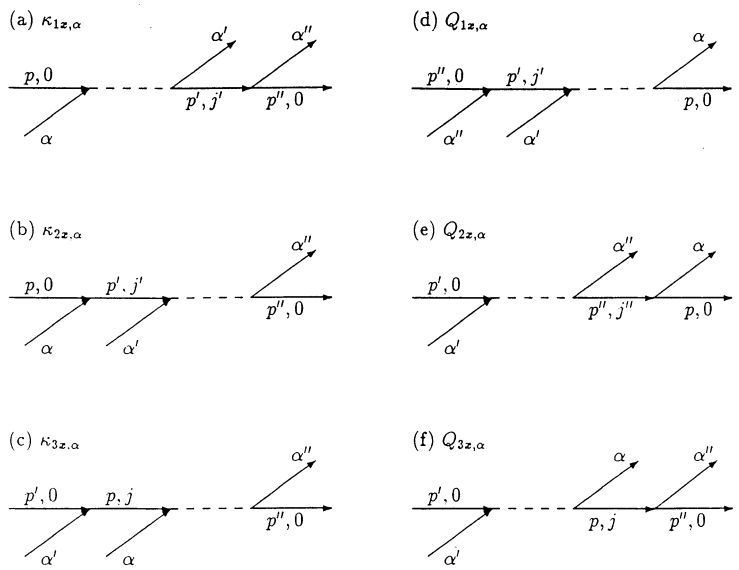

FIG. 2.—Compound diagrams for the two-photon scattering opacities and sources. Each involves two separate cross sections.

where $\bar{N}_\alpha$ is the equilibrium photon occupation number. Now in thermodynamic equilibrium, the occupation numbers are Planckian, and

$$\frac{n_{j'}(p')}{n_0(p)} = \exp\left[\frac{E_0(p) - E_{j'}(p')}{T}\right] = e^{(\omega' - \omega)/T} ,$$

where the last identity invokes energy conservation. Thus, the scattering cross sections are identical,

$$w_{0j'}(p, \alpha \to p', \alpha') = w_{j'0}(p', \alpha' \to p, \alpha) . \tag{12}$$

In a similar manner it is seen that, for absorption and emission,

$$w_{0j'}(p, \alpha \to p') = w_{j'0}(p' \to p, \alpha) . \tag{13}$$

The three opacity terms for the two-photon scattering are represented by the diagrams on the left-hand side of Figure 2. The first, $\chi_{1x,\alpha}$, is the direct process, while $\kappa_{2x,\alpha}$ and $\kappa_{3x,\alpha}$ represent the inverse and exchange. Although the diagrams in Figures 2*b* and 2*c* appear to be identical, they give different opacities, since to obtain the opacity for photon α, all other photon states are integrated. Following the diagram in Figure 2*a*, $\kappa_{1x,\alpha}$ is

$$\kappa_{1x,\alpha} = \int dp\, n_0(p) \int d\alpha' \sum_{j'} \int dp' w_{0j'}(p, \alpha \to p', \alpha')(1 + N_{\alpha'}) \frac{\int d\alpha'' \int dp'' w_{j'0}(p' \to p'', \alpha'')(1 + N_{\alpha''})}{\sum\limits_{j''' < j'} \int d\alpha''' \int dp''' w_{j'j'''}(p' \to p''', \alpha''')(1 + N_{\alpha'''})} , \tag{14}$$

where the $(1 + N_\alpha)$ factors account for stimulated scattering. The ratio in equation (14) is equal to unity, since the numerator is also integrated over all photons α'', however, for consistency in what follows, it will be kept. The stimulated factor in the denominator can be neglected with little loss in accuracy, and comparing this with equation (8), it is seen that

$$\kappa_{1x,\alpha} = \int d\alpha' \int d\alpha''(1 + k_{st} N_{\alpha''})(1 + k_{st} N_{\alpha'}) \mathcal{X}(\alpha \to \alpha'; \alpha'') , \tag{15}$$

where, as before $k_{st} = 1$ (0) to include (not include) stimulated scattering. Similarly, Figure 2*b* gives for $\kappa_{2x,\alpha}$,

$$\kappa_{2x,\alpha} = \int dp\, n_0(p) \int d\alpha' N_{\alpha'} \sum_{j'} \int dp' w_{0j'}(p, \alpha \to p') \frac{\int d\alpha'' \int dp'' w_{j'0}(p', \alpha' \to p'', \alpha'')(1 + N_{\alpha''})}{\sum\limits_{j''' < j'} \int d\alpha''' \int dp''' w_{j'j'''}(p' \to p''', \alpha''')(1 + N_{\alpha'''})} , \tag{16}$$

and using the detailed balance conditions and the fact that

$$n_0(p) = n_0(p'') \exp\left(\frac{E_0(p'') - E_0(p)}{T}\right) = e^{(\omega + \omega' - \omega'')/T} ,$$

by energy conservation for the entire process, $E_0(p) + \omega + \omega' = E_0(p'') + \omega''$, $\kappa_{2x,\alpha}$ can be written as

$$\kappa_{2x,\alpha} = \int d\alpha' \int d\alpha'' N_{\alpha'}(1 + N_{\alpha''}) e^{(\omega + \omega' - \omega'')/T} \int dp'' n_0(p'') \sum_{j'} \int dp' \int dp \frac{w_{0j'}(p'', \alpha'' \to p', \alpha') w_{j'0}(p' \to p, \alpha)}{\sum\limits_{j''' < j'} \int d\alpha''' \int dp''' w_{j'j'''}(p' \to p''', \alpha''')} . \tag{17}$$

© American Astronomical Society • Provided by the NASA Astrophysics Data System

1991ApJ...372..554A

Thus, $\kappa_{2x,\alpha}$ can also be written as an integral over the two-photon scattering redistribution function,

$$\kappa_{2x,\alpha} = \int d\alpha' \int d\alpha'' N_{\alpha'}(1 + k_{\rm st} N_{\alpha''}) e^{(\omega+\omega'-\omega'')/T} \mathcal{X}(\alpha'' \to \alpha'; \alpha) . \tag{18}$$

Finally, Figure 2*c* and the same steps give for $\kappa_{3x,\alpha}$,

$$\kappa_{3x,\alpha} = \int d\alpha' \int d\alpha'' N_{\alpha'}(1 + k_{\rm st} N_{\alpha''}) e^{(\omega'+\omega-\omega'')/T} \mathcal{X}(\alpha'' \to \alpha; \alpha') . \tag{19}$$

The processes that scatter photons into state α, i.e., the sources, are illustrated by the diagrams on the right-hand side in Figures 2*d*, 2*e*, and 2*f*. These may be expressed in terms of the two-photon scattering redistribution function in a manner identical to that for the opacities. Following steps analogous to those used for the opacities, we obtain the following expressions for the sources:

$$Q_{1x,\alpha} = (1 + k_{\rm st} N_\alpha) \int d\alpha' \int d\alpha'' N_{\alpha'} N_{\alpha''} e^{(\omega''+\omega'-\omega)/T} \mathcal{X}(\alpha \to \alpha'; \alpha'') , \tag{20}$$

$$Q_{2x,\alpha} = (1 + k_{\rm st} N_\alpha) \int d\alpha' \int d\alpha'' N_{\alpha'}(1 + k_{\rm st} N_{\alpha''}) \mathcal{X}(\alpha' \to \alpha''; \alpha) , \tag{21}$$

$$Q_{3x,\alpha} = (1 + k_{\rm st} N_\alpha) \int d\alpha' \int d\alpha'' N_{\alpha'}(1 + k_{\rm st} N_{\alpha''}) \mathcal{X}(\alpha' \to \alpha; \alpha'') . \tag{22}$$

2.3. *Two-Photon Emission*

The two-photon emission process, described by the compound diagram in Figure 1*d* for the special case where the initial electron is in $j = 0$, occurs when the electron absorbs a photon and is excited to a higher real state, from which it decays back in one jump with the emission of two photons. The two-photon emission redistribution function is constructed from the cyclotron absorption cross section and emission rate and the two-photon decay rate, and is defined in general as

$$\mathcal{Y}(\alpha \to \alpha'; \alpha'') \equiv \int dp\, n_j(p) \sum_{j'} \sum_{j''<j'} \int dp' \frac{\int dp'' w_{jj'}(p, \alpha \to p') w_{j'j''}(p' \to p'', \alpha', \alpha'')}{\sum_{j'''<j'} \int d\alpha''' \int dp''' w_{j'j'''}(p' \to p''', \alpha''')} . \tag{23}$$

This expression can be interpreted as the integrated $j \to j'$ absorption rate times the probability that the excited electron will spontaneously decay by emitting two photons α' and α'' instead of a single photon α'''. As before, we shall not discuss decays to an excited state, which would result in a third photon out. The necessary rates to construct $\mathcal{Y}(\alpha \to \alpha'; \alpha'')$ are contained in the Appendix, and the integrations and angle averages proceed in a similar manner to those used for $\mathcal{X}(\alpha \to \alpha'; \alpha'')$. The result, for the case $j = j'' = 0$ is

$$\begin{aligned}\mathcal{Y}(\alpha \to \alpha'; \alpha'') = \pi r_0^2 \frac{\omega'\omega''}{\omega} \sum_{j'} \sum_{p_\pm} n_0(p_\pm) \frac{m^2(E+m)(E'+m)(E''+m)}{[(\Delta + 2m\omega_c j')^2 + 4\Delta m^2]^{1/2} E''} \Bigg|_{\substack{p'=p+k \\ p''=p'-k'-k''}} \\ \times \sum_{j_i} \left[|c_{j_i}|^2 + |d_{j_i}|^2 + 2(-1)^{j_i} \sum_{j_3} (-1)^{j_3} J_{j_i+j_3-j'}(2\sqrt{\xi'\xi''}) \,\mathrm{Re}\,(c_{j_i} d_{j_3}^*) \right] \\ \times \delta(E'' + \omega'' + \omega' - E') |\boldsymbol{\epsilon} \cdot \boldsymbol{G}^*_{\beta\beta'}(-\boldsymbol{k}_\perp)|^2 \Bigg/ \left[\sum_{j'''<j'} \sum_{\epsilon'''} \int_{-1}^{1} d\mu''' \frac{\tilde{\omega}(E''' + m)}{E'''} |\boldsymbol{\epsilon}'''^* \cdot \boldsymbol{G}_{\beta'''\beta'}(-\tilde{\boldsymbol{k}}_\perp)|^2 \right] ,\end{aligned} \tag{24}$$

where here $p_\pm$ is given by equation (3) with $\omega' = k' = 0$ and $\Delta = k^2 - \omega^2$, and the decay frequency, $\tilde{\omega}$, is given by equation (10).

Previously, it was seen that the two-photon scattering process and its inverse and exchange give three opacities and three sources. The same is true here. Again, with the use of the detailed balance conditions for the scattering rates, all of the opacities and sources may be expressed as integrals of the redistribution function. The necessary detailed balance conditions are

$$w_{0j'}(p \to p', \alpha, \alpha') = w_{j'0}(p', \alpha, \alpha' \to p)$$

and

$$w_{0j'}(p, \alpha \to p') = w_{j'0}(p' \to p, \alpha) .$$

The steps in obtaining the opacities and sources as integrals over $\mathcal{Y}(\alpha \to \alpha'; \alpha'')$ are identical with those used in the previous section, so here just the final expressions are presented.

The diagrams that represent the opacity terms for the two-photon emission process are shown in Figures 3*a*, 3*b*, and 3*c*, and the corresponding integral expressions are

$$\kappa_{1y,\alpha} = \int d\alpha' \int d\alpha''(1 + k_{\rm st} N_{\alpha'})(1 + k_{\rm st} N_{\alpha''}) \mathcal{Y}(\alpha \to \alpha'; \alpha'') , \tag{25}$$

$$\kappa_{2y,\alpha} = \int d\alpha' \int d\alpha'' N_{\alpha'}(1 + k_{\rm st} N_{\alpha''}) e^{(\omega+\omega'-\omega'')/T} \mathcal{Y}(\alpha'' \to \alpha; \alpha') , \tag{26}$$

$$\kappa_{3y,\alpha} = \int d\alpha' \int d\alpha'' N_{\alpha'}(1 + k_{\rm st} N_{\alpha''}) e^{(\omega'+\omega-\omega'')/T} \mathcal{Y}(\alpha'' \to \alpha'; \alpha) . \tag{27}$$

© American Astronomical Society • Provided by the NASA Astrophysics Data System

1991ApJ...372..554A

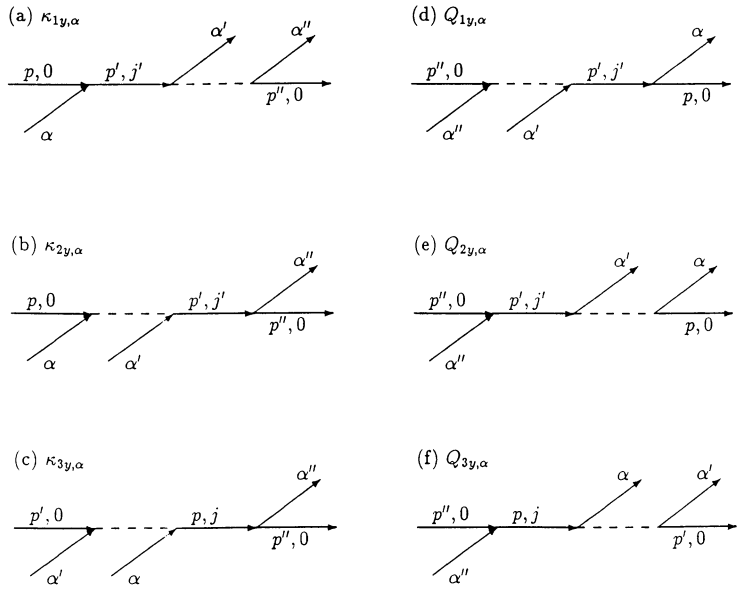

FIG. 3.—Compound diagrams for the two-photon emission opacities and sources

The diagrams that illustrate the source terms for two-photon emission are shown in Figures 3*d*, 3*e*, and 3*f*. These give the following integrals:

$$Q_{1y,\alpha} = (1 + k_{st} N_\alpha) \int d\alpha' \int d\alpha'' N_{\alpha'} N_{\alpha''} e^{(\omega' + \omega'' - \omega)/T} \mathcal{Y}(\alpha \to \alpha'; \alpha'') , \tag{28}$$

$$Q_{2y,\alpha} = (1 + k_{st} N_\alpha) \int d\alpha' \int d\alpha'' N_{\alpha''} (1 + k_{st} N_{\alpha'}) \mathcal{Y}(\alpha'' \to \alpha'; \alpha) , \tag{29}$$

$$Q_{3y,\alpha} = (1 + k_{st} N_\alpha) \int d\alpha' \int d\alpha'' N_{\alpha''} (1 + k_{st} N_{\alpha'}) \mathcal{Y}(\alpha'' \to \alpha; \alpha') . \tag{30}$$

It should be pointed out that these results are valid for an arbitrary distribution of electrons, thermal or nonthermal. The condition of detailed balance requires a thermal distribution; however, this is used only to relate a scattering rate to its inverse.

3. RESULTS FOR THERMAL DISTRIBUTIONS

In this section we present the numerical results of calculations of the cross sections that were derived in the previous section for a thermal distribution. For all of the calculations, the plasma conditions are those that will be used to simulate the atmosphere of the accreting X-ray pulsar Hercules X-1 (e.g., Mészáros & Nagel 1985a). These are cyclotron energy, $\omega_c = 38$ keV; temperature, $T = 8$ keV; and density, $\rho = 0.5$ g cm^{-3} (the latter two are not necessarily unique). In addition, the polarization vectors are calculated by the techniques in Bussard, Lamb, & Packey (1986), who employ the methods of Pavlov, Shibanov, & Yakovlev (1980). Briefly, the method determines the fully relativistic polarization tensor for a hot plasma in a strong magnetic field. From this, the complex indices of refraction and the normal-mode eigenvectors are calculated for given photon energy and direction. The polarizability of the plasma electrons and the effects of vacuum polarization are included in the limit where $B/B_{crit} = \hbar\omega_c/mc^2 \ll 1$. This is the method that is employed throughout this work to calculate the polarization vectors. For the calculations in this paper, stimulated processes are ignored throughout (i.e., $k_{st} = 0$).

Figure 4 shows plots of the one-photon opacity and source cross sections normalized to the field-free Thomson cross section ($\sigma_T = 8\pi r_0^2/3$), where a Wien (i.e., $N_\alpha = e^{-\omega/T}$) distribution of photons is assumed to calculate $Q_{C,\alpha}$. For this calculation, the summation over intermediate electron states was carried out for $j'' = 0, 1, 2, 3$. Thus the cross section includes effects up to the third cyclotron harmonic, aside from any small corrections associated with three-photon processes or higher order effects. In addition, these plots (as are all of the plots in this paper) are for an incident photon angle of 60° relative to the external magnetic field. The cross sections differ from the total cross sections in BAM in that here $\kappa_{C,\alpha}$ contains only terms where the final electron is in the ground state. The cross sections in BAM actually represent the sum of the one-photon scattering, $\kappa_{C,\alpha}$, and the direct two-photon scattering process, $\kappa_{1x,\alpha}$. (The other processes, $\kappa_{2x,\alpha}$, $\kappa_{3x,\alpha}$, and the two-photon emission, were not considered in BAM.)

The cross sections are plotted for the two normal polarization modes that are labeled ordinary (O) and extraordinary (X). In the limit of low photon energy, where vacuum effects are negligible, this gives the convention that ordinary (extraordinary) photons propagating transverse to the external field have their electric field vector parallel (perpendicular) to the external field, or for photons propagating longitudinally to the external field, ordinary (extraordinary) photons have an electric field vector rotating in the opposite (same) sense as the gyration of an electron in the magnetic field. Thus, in this limit, the extraordinary photon sees a tightly bound electron, while the ordinary photon sees virtually a free electron. As the first cyclotron harmonic is approached, vacuum effects cause scattering between the modes, and both become resonant.

© American Astronomical Society • Provided by the NASA Astrophysics Data System

1991ApJ...372..554A

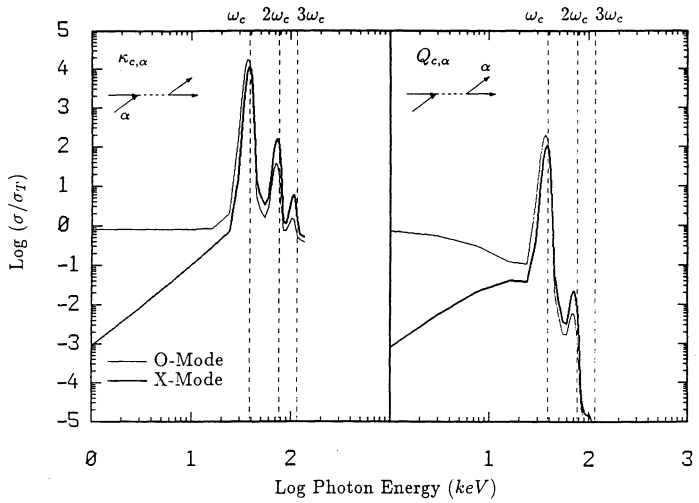

FIG. 4.—Opacity and source cross sections for one-photon scattering for the following plasma parameters: cyclotron frequency, $\omega_c = 38$ keV; temperature, $T = 8$ keV; and density, $\rho = 0.5$ g cm^{-3}. The incident photon angle is 60° relative to the external field.

Previous calculations of one-photon Compton scattering have been nonrelativistic and have not included the higher cyclotron harmonics (see, e.g., Nagel 1981 or Mészáros & Nagel 1985a). Including relativistic effects causes the resonant frequencies to be slightly less than the integral multiples of ω_c. These resonances are correctly given by

$$\omega = (-m + \sqrt{m^2 + 2m\omega_c n \sin^2\theta})/\sin^2\theta ,$$

where n labels the Landau or harmonic level. This shift is present in Figure 4. In addition, including the higher harmonics causes a faster decrease in the high-energy wing of the first cyclotron resonance than is seen in previous calculations (cf. Mészáros et al. 1984).

The cross sections for the two-photon scattering can be calculated in a manner similar to that used for the one-photon cross sections. The redistribution function, $\mathcal{R}(\alpha \to \alpha'; \alpha'')$, is calculated for a set of photon frequencies, directions, and two polarization modes. Then the various integrals of $\mathcal{R}(\alpha \to \alpha'; \alpha'')$ give the required opacities and sources. For all of these calculations, the plasma conditions are identical to those used for one-photon scattering, stimulated factors are neglected throughout, and a Wien photon distribution is used wherever the cross section depends on the occupation number.

Figure 5 shows the two-photon scattering opacity and source cross sections $\kappa_{1x,\alpha}$ and $Q_{1x,\alpha}$ calculated from equations (15) and (20). The opacity cross section is zero until the photon has sufficient energy to scatter the electron into the first excited state, $j' = 1$, with the scattered photon, ω', having low energy. The electron then decays to the ground state with the emission of photon ω''. This excitation has a weak resonance that peaks near ω_c. When the initial photon has sufficient energy to scatter the electron into either the $j' = 2$ or the $j' = 3$ level, strong resonances occur in the cross section at $\omega \sim 2\omega_c$ and $3\omega_c$. Comparing these plots with Figure 4 for the one-photon scattering cross sections, we see that in the vicinity of the second and third cyclotron harmonic, the two-photon

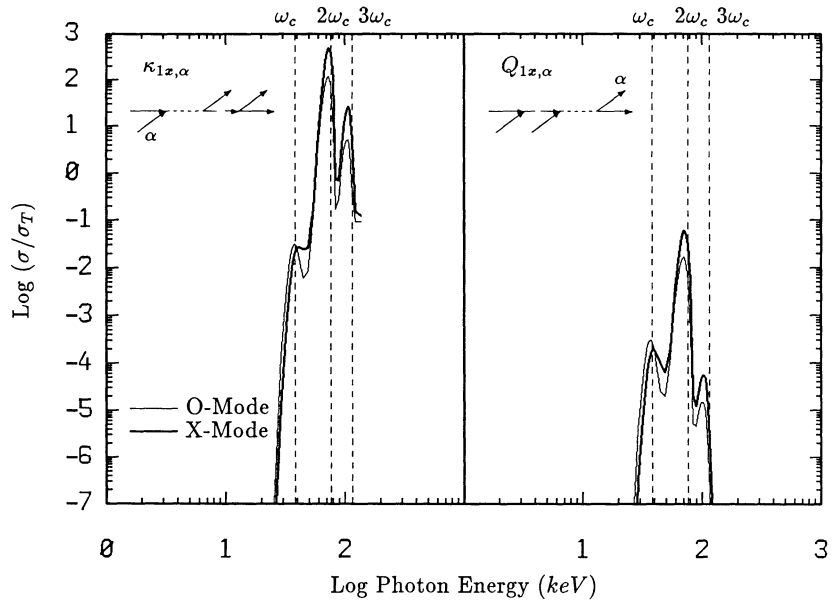

FIG. 5.—Two-photon scattering opacities and source cross sections, $\kappa_{1x,\alpha}$ and $Q_{1x,\alpha}$, for the same conditions as in Fig. 4

© American Astronomical Society • Provided by the NASA Astrophysics Data System

1991ApJ...372..554A

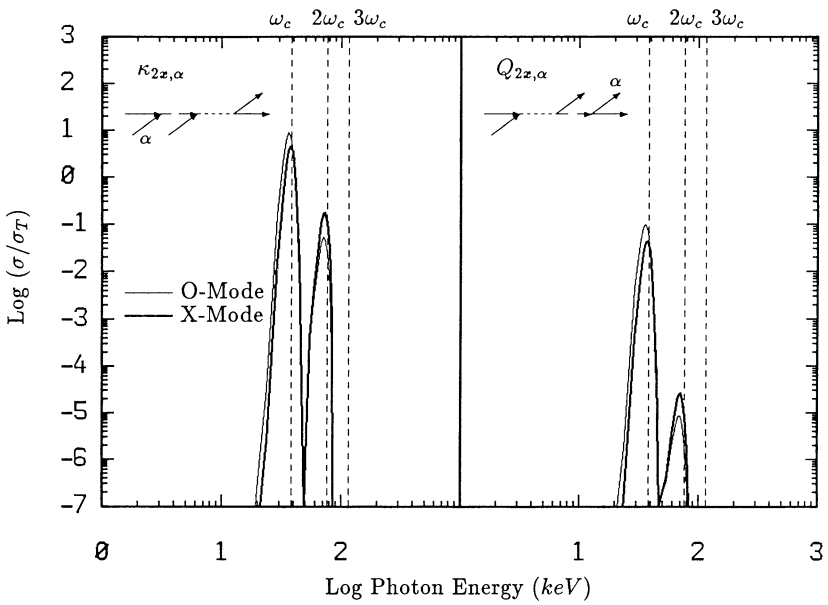

FIG. 6.—Two-photon scattering opacities and source cross sections, $\kappa_{2x,\alpha}$ and $Q_{2x,\alpha}$, for the same conditions as in Fig. 4

scattering cross section exceeds the one-photon by large factors near $\omega \sim 2\omega_c$ and $\omega \sim 3\omega_c$. Evidently, if the higher level harmonics are to be studied, the two-photon scattering must be included.

The opacity and source cross sections for the inverse and exchange two-photon scattering, $\kappa_{2x,\alpha}$, $Q_{2x,\alpha}$ and $\kappa_{3x,\alpha}$, $Q_{3x,\alpha}$, are shown in Figures 6 and 7, respectively. All of these cross sections exhibit resonances near ω_c and $2\omega_c$ that are quite small compared with those for either $\kappa_{1x,\alpha}$ or $\kappa_{C,\alpha}$. Figure 6 shows that $\kappa_{2x,\alpha}$ is similar to a pure absorption cross section in that it is zero for energies insufficient to cause the electron to be lifted to the first excited state. This is consistent with the diagram for $\kappa_{2x,\alpha}$ in Figure 2*b*. On the other hand, Figure 7 shows that $\kappa_{3x,\alpha}$ is nonzero at low photon energies. This is expected from the diagram in Figure 2*c* which shows that for $\kappa_{3x,\alpha}$ the photon α scatters from an excited-state electron, which is energetically possible for low photon energy.

The two-photon emission redistribution function can be calculated for the same conditions as for the two-photon scattering. Then the prescribed integrals give the opacities and sources. Figures 8, 9, and 10 show plots of the two-photon emission opacity and source cross sections. We see in Figure 8 that $\kappa_{1y,\alpha}$ shows the form of a pure absorption, i.e., zero for energies insufficient to excite the electron. However, the heights of the resonances at the higher harmonics reveal that this process is much more efficient for photon energies above the fundamental. For $\kappa_{1y,\alpha}$, the cross section near the second and third harmonics is not as large as that for $\kappa_{1x,\alpha}$, but still larger than that for one-photon scattering. Resonances beyond the third harmonic would be present if the range of frequencies were extended. The diagrams for $\kappa_{2y,\alpha}$ and $\kappa_{3y,\alpha}$ are identical except for an interchange of photons α and α'. This identity is apparent

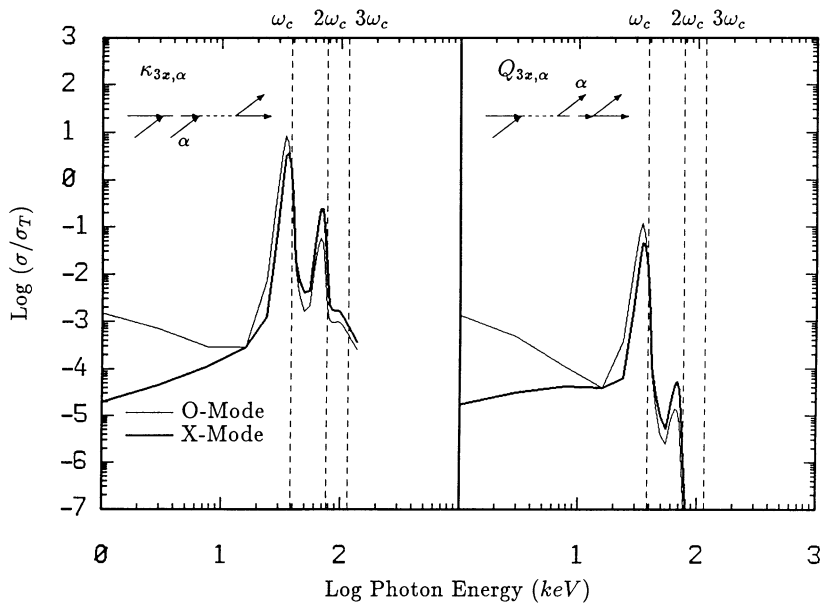

FIG. 7.—Two-photon scattering opacities and source cross sections, $\kappa_{3x,\alpha}$ and $Q_{3x,\alpha}$, for the same conditions as in Fig. 4

© American Astronomical Society • Provided by the NASA Astrophysics Data System

1991ApJ...372..554A

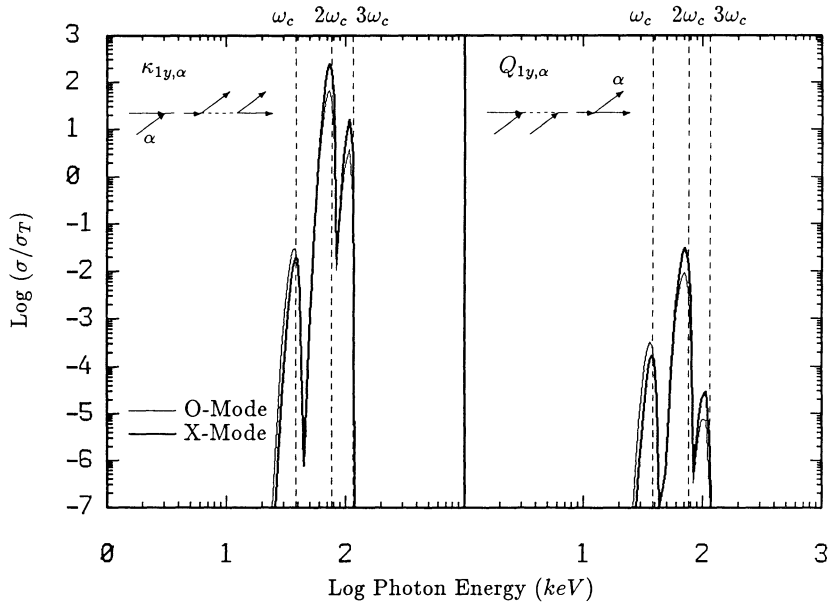

FIG. 8.—Two-photon emission opacities and source cross sections, $\kappa_{1y,\alpha}$ and $Q_{1y,\alpha}$, for the same conditions as in Fig. 4

in the plots in Figures 9 and 10. Both $\kappa_{2y,\alpha}$ and $K_{3y,\alpha}$ are nonzero for low energy, since the other photon, α' may have sufficient energy to cause the excitation.

4. DISCUSSION

We have presented a systematic description of all the electron radiative processes in a magnetic field which are of second order in the fine-structure constant. The first-order diagrams are also included, insofar as the radiative excitation to and radiative decay from an excited mass shell (real) electron state is part of the one-photon processes, neglecting the much more infrequent case of collisional excitation and de-excitation. All the possible Feynman diagrams have been considered, with the various permutations and ordering of photons and electrons, which is necessary in QED. This is necessary for determining in a quantitative way the relative importance of the various mechanisms, a knowledge of which is necessary for performing model radiative transfer calculations.

The values of the opacities and sources calculated in § 3, while calculated for a specific choice of plasma parameters typical for accreting pulsars, give an idea of the order-of-magnitude relation between the various radiative processes described in Figure 1. The first thing that stands out is a verification of the qualitative statement made in § 1, namely, that the one-photon scattering $\kappa_{C,\alpha}$ (Figs. 1*a* and 4) is roughly comparable to the direct two-photon scattering $\kappa_{1x,\alpha}$ (Figs. 2*a* and 5). At the first harmonic, the two-photon scattering makes only a small correction, but at the higher harmonics the two-photon processes are dominant. The inverse

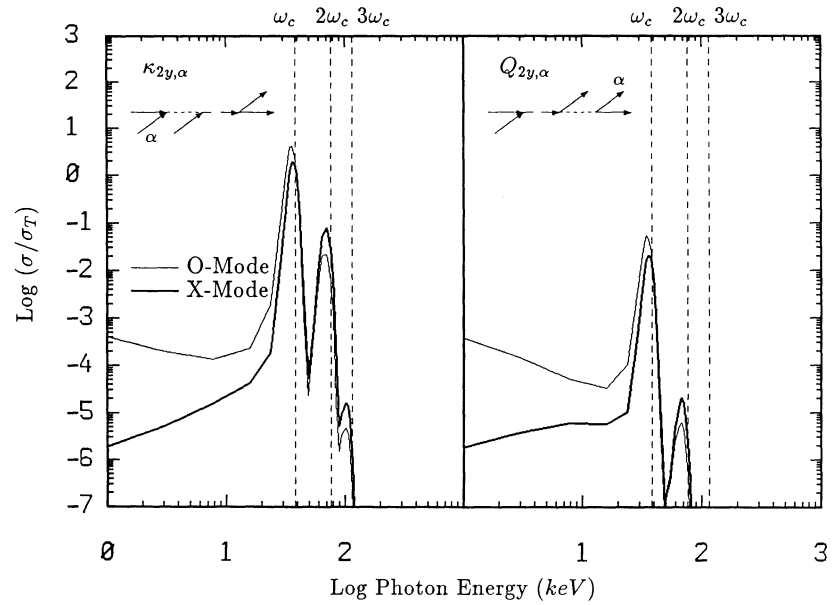

FIG. 9.—Two-photon emission opacities and source cross sections, $\kappa_{2y,\alpha}$ and $Q_{2y,\alpha}$, for the same conditions as in Fig. 4

© American Astronomical Society • Provided by the NASA Astrophysics Data System

1991ApJ...372..554A

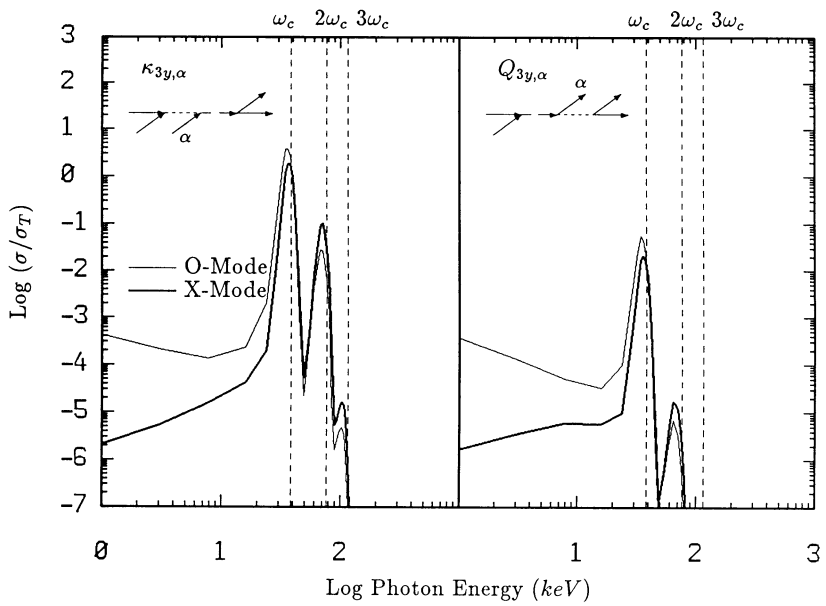

FIG. 10.—Two-photon emission opacities and source cross sections, $\kappa_{3y,\alpha}$ and $Q_{3y,\alpha}$, for the same conditions as in Fig. 4

two-photon processes $\kappa_{2x,\alpha}$, $\kappa_{3x,\alpha}$ of Figures 6 and 7 also dominate the single-photon scattering at the high harmonics, although not the direct two-photon scattering $\kappa_{1x,\alpha}$ of Figure 5. One might naively think that this would allow one to neglect $\kappa_{2x,\alpha}$, $\kappa_{3x,\alpha}$ with respect to $\kappa_{1x,\alpha}$, and indeed this may be to some degree acceptable in an optically thin calculation. However, if the optical thickness to scattering is moderate or high, they must be included, otherwise the radiation field will not tend to a thermal equilibrium distribution as required. The same applies for the corresponding source terms, shown in the right-hand panel of Figures 4–7. For high optical depth plasmas, if the temperature or input spectrum is such that higher harmonics will enter the picture, it is inconsistent to include the one-photon scattering without also including all the two-photon scattering processes as well.

Consider now the two-photon emission process of Figures 1*d* and 3. Comparing the direct two-photon emission following radiative excitation $\kappa_{1y,\alpha}$ (Fig. 8) with the direct two-photon scattering $\kappa_{1x,\alpha}$ (Fig. 5), one sees that the former is somewhat smaller than the latter at the line cores, and both are much larger at the higher harmonics than the single-photon scattering of $\kappa_{C,\alpha}$ of Figure 4. However, the two-photon emission $\kappa_{1y,\alpha}$ has no continuum contribution. Therefore, even in an optically thin situation, all three of these processes must be included simultaneously. On the other hand, the inverse processes of two-photon absorption followed by radiative decay $\kappa_{2y,\alpha}$, $\kappa_{3y,\alpha}$ (Fig. 9) are comparable in strength to the two-photon inverse processes $\kappa_{2x,\alpha}$, $\kappa_{3x,\alpha}$ of Figures 6 and 7. These processes therefore may also be neglected in an optically thin situation, but must be included together with all the others in a self-consistent treatment, especially if the atmosphere is optically thick. Their neglect could otherwise lead to spurious effects, such as a spectral density exceeding blackbody or unduly below blackbody, in those spectral regions where the opacity is very large, e.g., at low frequencies or near the cyclotron resonances.

In conclusion, we have presented a QED treatment of the one- and two-photon magnetic scattering cross sections and redistributions, and we have introduced the magnetic two-photon emission opacity and redistribution function. We have also discussed the corresponding inverse processes, including all possible permutations of photons and vertices. We have investigated the details of the two-photon emission process, which is of the same order but somewhat weaker than the two-photon scattering. These cross sections and redistribution functions are useful in modeling quantitatively the spectra of accreting pulsars and gamma-ray bursters.

We are grateful to Roger W. Bussard for advice concerning the two-photon cross-section formalism and to Alice Harding and John Wang for valuable comments. This research has been supported in part through grants NASA NAGW-1522 and NSF AST 8815266.

APPENDIX

The differential cross section for Compton scattering in a strong magnetic field has been derived from quantum electrodynamics in BAM. For electrons characterized by an energy E, momentum component parallel to the external field, p, and total magnetic quantum number $j = n + s + \frac{1}{2}$, and photons given by energy ω, wavevector $\boldsymbol{k}$, and polarization unit vector $\boldsymbol{\varepsilon}$ (note that $\hbar = c = 1$ units are used throughout), the differential cross section for Compton scattering is

$$w_{jj'}(\boldsymbol{k}, \boldsymbol{\varepsilon}, p \to \boldsymbol{k}', \boldsymbol{\varepsilon}', p') = \frac{e^4}{\omega\omega'}\left(\frac{E+m}{2E}\frac{E'+m}{2E'}\right)\delta(E' + \omega' - E - \omega)\delta(p' + k' - p - k)$$

$$\times \left|\sum_{j''}(a_{j''}e^{ij''(\phi'-\phi)} + b_{j''}e^{-ij''(\phi'-\phi)}e^{2i\Delta})\right|^2 d^3k'\,dp' , \quad \text{(A1)}$$

© American Astronomical Society • Provided by the NASA Astrophysics Data System

1991ApJ...372..554A

where unprimed quantities refer to the initial values, primed ones to the final values, and double-primed ones to the intermediate electron states. Also, in equation (A1)

$$a_{j''} = \frac{E''+m}{2E''} \sum_{s'',\lambda''} \frac{[\boldsymbol{\varepsilon}'^* \cdot \boldsymbol{G}_{\beta'\beta''}(-\boldsymbol{k}'_\perp)][\boldsymbol{\varepsilon} \cdot \boldsymbol{G}^*_{\beta\beta''}(-\boldsymbol{k}_\perp)]}{E+\omega-\lambda''(E''-(i/2)\Gamma_{\beta''})}\bigg|_{p''=p+k}, \tag{A2}$$

$$b_{j''} = \frac{E''+m}{2E''} \sum_{s'',\lambda''} \frac{[\boldsymbol{\varepsilon} \cdot \boldsymbol{G}^*_{\beta''\beta'}(-\boldsymbol{k}_\perp)][\boldsymbol{\varepsilon}^* \cdot \boldsymbol{G}_{\beta''\beta}(-\boldsymbol{k}'_\perp)]}{E-\omega'-\lambda''(E''-(i/2)\Gamma_{\beta''})}\bigg|_{p''=p-k'}, \tag{A3}$$

$$\Lambda = \frac{j+j'}{2}(\phi'-\phi) + \sqrt{\xi\xi'}\sin(\phi'-\phi). \tag{A4}$$

where ϕ is the azimuthal angle of the photon direction, $\xi = k_\perp^2/2m\omega_c$, and the components of the vector $\boldsymbol{G}$ depend on spin and are defined in BAM. [Note that in BAM, $w_{jj'}(\boldsymbol{k}, \boldsymbol{\varepsilon}, p \to \boldsymbol{k}', \boldsymbol{\varepsilon}', p')$ is referred to as a rate; however, it is actually a cross section.]

Also necessary for the construction of the redistribution functions for the two-photon processes are the cyclotron absorption cross section and decay rate. These were first derived in Daugherty & Ventura (1978) and Bussard (1980), and in the same nomenclature used for the Compton scattering the absorption cross section is

$$w_{jj'}(p; \boldsymbol{k}, \boldsymbol{\varepsilon} \to p') = \frac{(2\pi)^2 e^2}{\omega}\delta(E'-\omega-E)\delta(p'-k-p)\left[\frac{(E+m)(E'+m)}{4EE'}\right]|\boldsymbol{\varepsilon} \cdot \boldsymbol{G}^*_{\beta\beta'}(-\boldsymbol{k}_\perp)|^2 dp' \tag{A5}$$

and the cyclotron emission rate for an electron in an excited state is

$$w_{jj'}(p \to \boldsymbol{k}, \boldsymbol{\varepsilon}; p') = \frac{e^2}{2\pi\omega}\delta(E'+\omega-E)\delta(p'+k-p)\left[\frac{(E+m)(E'+m)}{4EE'}\right]|\boldsymbol{\varepsilon}^* \cdot \boldsymbol{G}_{\beta'\beta}(-\boldsymbol{k}_\perp)|^2 dp'\, d^3k. \tag{A6}$$

The final quantity required to construct the redistribution functions is the two-photon decay rate for an excited electron to decay to a lower energy level with the emission of two photons instead of one. This rate can be derived from S-matrix theory in an identical manner to that used to arrive at equation (A1). In fact, the only difference here is that both photons are emitted, which can be accounted for as a crossing symmetry by replacing the wavevector for the incident photon with $\boldsymbol{k} \to -\boldsymbol{k}$ and the corresponding azimuth angle by $\phi \to \phi + \pi$. The resulting rate for two-photon decay can be written in a form analogous to Compton scattering:

$$w_{jj'}(p \to \boldsymbol{k}, \boldsymbol{\varepsilon}; \boldsymbol{k}, \boldsymbol{\varepsilon}'; p') = \frac{e^4}{(2\pi)^3\omega\omega'}\left[\frac{E+m}{2E}\frac{E'+m}{2E'}\right]\delta(E'+\omega'+\omega-E)\delta(p'+k'+k-p)$$
$$\times\left|\sum_{j''}(c_{j''}e^{ij''(\phi'-\phi)} + d_{j''}e^{-ij''(\phi'/\phi)}e^{2i\Lambda_2})\right|^2 d^3k\, d^3k'\, dp', \tag{A7}$$

where for the case of two-photon decay

$$c_{j''} = (-1)^{j''}\frac{E''+m}{2E''}\sum_{s'',\lambda''}\frac{[\boldsymbol{\varepsilon}'^* \cdot \boldsymbol{G}_{\beta'\beta''}(-\boldsymbol{k}'_\perp)][\boldsymbol{\varepsilon}^* \cdot \boldsymbol{G}_{\beta''\beta}(-\boldsymbol{k}_\perp)]}{E-\omega-\lambda''(E''-(i/2)\Gamma_{\beta''})}\bigg|_{p''=p-k}, \tag{A8}$$

$$d_{j''} = (-1)^{j}\frac{E''+m}{2E''}\sum_{s'',\lambda''}\frac{[\boldsymbol{\varepsilon}^* \cdot \boldsymbol{G}_{\beta'\beta''}(-\boldsymbol{k}_\perp)][\boldsymbol{\varepsilon}'^* \cdot \boldsymbol{G}_{\beta''\beta}(-\boldsymbol{k}'_\perp)]}{E-\omega'-\lambda''(E''-(i/2)\Gamma_{\beta''})}\bigg|_{p''=p-k'}, \tag{A9}$$

$$\Lambda_2 = \frac{j+j'}{2}(\phi'-\phi-\pi) + \sqrt{\xi\xi'}\sin(\phi'-\phi). \tag{A10}$$

REFERENCES

Alexander, S. G., & Mészáros, P. 1989, ApJ, 344, L1
———. 1990a, BAAS, 21, (No. 4), 1175
———. 1990b, ApJ, 372, 565
Alexander, S. G., Mészáros, P., & Bussard, R. W. 1989, ApJ, 342, 928
Bussard, R. W. 1980, ApJ, 237, 970
Bussard, R. W., Alexander, S. G., & Mészáros, P. 1986, Phys. Rev. D, 34, 440 (BAM)
Bussard, R., & Lamb, F. K. 1982, in AIP Conf. Proc. 115, High Energy Transients in Astrophysics, ed. S. Woosley (New York: AIP), 189
Bussard, R. W., Lamb, F. K., & Packey, D. 1986, Marshall Space Flight Center Rept. No. 86-130, unpublished
Bussard, R. W., Mészáros, P., & Alexander, S. G. 1985, ApJ, 297, L21
Clark, G. W., Woo, J. W., Nagase, F., Makishima, K., & Sakao, T. 1990, ApJ, 353, 274
Daugherty, J., & Harding, A. K. 1986, ApJ, 309, 362
Daugherty, J., & Ventura, J. 1978, Phys. Rev. D, 18 (No. 4), 1053
Herold, H. 1979, Phys. Rev. D, 19, 2868
Harding, A. K., & Preece, R. 1989, ApJ, 338, L21
Mazets, E. P., et al. 1982, Nature, 290, 378
Melrose, D., & Kirk, J. G. 1986, A&A, 156, 268
Mészáros, P., and Bussard, R. W. 1984, in AIP Conf. Proc. 141, Gamma-Ray Bursts, ed. E. P. Liang and V. Petrosian (New York: AIP), 121
Mészáros, P., & Nagel, W. 1985a, ApJ, 298, 147
Murakami, T., et al. 1988, Nature, 335, 234
Nagase, F. 1989, in Proc. 23d ESLAB Symposium on X-Ray Astronomy (Bologna), ed. J. Hunt & B. Battrick (ESA SP-296), 45
Nagel, W. 1981, ApJ, 251, 288
Pavlov, G. G., Shibanov, Yu. A., & Yakovlev, D. G. 1980, Ap&SS, 73, 33
Trümper, J., et al. 1978, ApJ, 219, L105
Wang, J. C., et al. 1989, Phys. Rev. Letters, 63, 1550
White, N. E., Swank, J. H., & Holt, S. S. 1983, ApJ, 270, 711

© American Astronomical Society • Provided by the NASA Astrophysics Data System